Synthesis, structure and catecholase activity study of dinuclear copper(II) complexes †

Jörg Reim and Bernt Krebs *

Anorganisch-Chemisches Institut der Universität Münster, Wilhelm-Klemm-Strasse 8, D-48149 Münster, Germany

A series of dinuclear copper(II) complexes as models for the type 3 copper protein catechol oxidase were synthesised. They were characterised by spectroscopic, electrochemical, and in some cases, by single-crystal X-ray diffraction studies: $[Cu_2(L^1)(OH)(EtOH)(H_2O)][ClO_4]_2 \cdot H_2O$ **1**, $[Cu_2(L^2)(OH)][NO_3]_2$ **2**, $[Cu_2(L^3)(OMe)(MeOH)(ClO_4)]ClO_4$ **3**, $[Cu_2(L^4)(OH)(MeOH)_2][BF_4]_2$ **4**, $[Cu_2(L^5)(OMe)][ClO_4]_2 \cdot 2MeOH$ **5**, $[Cu_2(L^6)(OMe)(MeOH)(ClO_4)]ClO_4$ **6** and $[Cu_2(L^7)(OMe)(MeOH)(ClO_4)]ClO_4$ **7** (HL^1 = 4-bromo-2,6-bis(4-methylpiperazin-1-ylmethyl)-phenol, HL^2 = 4-bromo-2,6-bis[[2-pyridylmethyl)aminomethyl]phenol, HL^3 = 4-bromo-2,6-bis{[2-(2-pyridyl)-ethyl]aminomethyl}phenol, HL^4 = 4-bromo-2,6-bis{[2-(1-methyl-2-imidazolyl)ethyl]aminomethyl}phenol, HL^5 = 4-bromo-2-(4-methylpiperazin-1-ylmethyl)-6-[(2-pyridylmethyl)aminomethyl]phenol, HL^6 = 4-bromo-2-(4-methylpiperazin-1-ylmethyl)-6-{[2-(2-pyridyl)ethyl]aminomethyl}phenol and HL^7 = 4-bromo-2-(4-methyl-piperazin-1-ylmethyl)-6-{[2-(1-methyl-2-imidazolyl)ethyl]aminomethyl}phenol). The copper centres are μ-phenoxo bridged by the pentadentate dinucleating ligand and exogenously μ-hydroxo or μ-methanolato bridged. Complex **1** crystallises in $P2_1/c$ with a = 16.913(3), b = 11.046(2), c = 16.617(3) Å, β = 94.06(3)°, U = 3097 Å^3 and Z = 4. Complex **3** crystallises in $P2_1/n$ with a = 10.592(2), b = 12.123(2), c = 24.482(5) Å, β = 92.97(3)°, U = 3139 Å^3 and Z = 4. Complex **4** crystallises in $Pbcn$ with a = 16.043(3), b = 12.689(3), c = 15.810(3) Å, U = 3218 Å^3 and Z = 4. Complex **6** crystallises in $P2_1/c$ with a = 17.889(4), b = 10.401(2), c = 16.269(4) Å, β = 92.94(2)°, U = 3023 Å^3 and Z = 4. Complex **7** crystallises in $P2_1/c$ with a = 17.349(3), b = 8.828(2), c = 19.797(4) Å, β = 94.04(3)°, U = 3025 Å^3 and Z = 4. A catecholase activity study revealed that only complexes **1**, **5**, **6** and **7** have significant catalytic activity with respect to the aerial oxidation of 3,5-di-*tert*-butylcatechol. A kinetic treatment on the basis of the Michaelis–Menten model was applied.

The oxidation of organic substrates with molecular oxygen under mild conditions is of great interest for industrial and synthetic processes both from an economical and environmental point of view.[1] Although the reaction of organic substances with dioxygen is thermodynamically favoured, it is kinetically unfavoured due to the triplet ground state of O_2. In biological systems this problem is overcome by the use of copper- or iron-containing metalloproteins which serve as highly efficient oxidation catalysts.[2] The synthesis and investigation of functional model complexes for metalloenzymes with oxidase or oxygenase activity is therefore of great promise for the development of new and efficient catalysts for oxidation reactions.

Type 3 copper proteins are characterised by a dinuclear copper active site which is antiferromagnetically coupled in the oxidised state and therefore EPR silent.[2,3] Well known representatives of type 3 copper proteins are hemocyanin,[4] the dioxygen carrier for arthropods and mollusks, and tyrosinase,[5] which catalyses the hydroxylation of tyrosine to dopa [3-(3,4-dihydroxyphenyl)alanine] (cresolase activity) and the oxidation of dopa to dopaquinone (catecholase activity). In contrast to tyrosinase, other copper-containing polyphenol oxidases only catalyse the aerial oxidation of *o*-diphenols (catechols) to the corresponding *o*-quinones without acting on tyrosine.[6] This reaction is of great importance in medical diagnosis for the determination of the hormonally active catecholamines adrenaline, noradrenaline and dopa.[7] X-Ray absorption spectroscopy investigations on the native met forms of catechol oxidases (EC 1.10.3.1) from *Lycopus europaeus* and *Ipomoea batatas* have revealed that the active site consists of a dicopper(II) centre, where the metal atoms are co-ordinated by four N/O donor ligands.[8] Multiple scattering calculations have shown a high significance for one or two co-ordinating histidine residues.[8c] The short metal–metal distance of 2.9 Å and the results of EPR investigations indicate a di-μ-hydroxo bridged dicopper(II) active site in the met forms of the proteins.[8]

The catecholase activity of copper co-ordination compounds with different structural parameters has been investigated to some extent.[9] In these studies mono- or multi-nuclear complexes have been employed and the properties of the chelating ligands with respect to architecture, number and nature of the donor atoms have been varied. Nishida and co-workers[9a] have found that square-planar mononuclear copper(II) complexes exhibit only little catalytic activity while non-planar mononuclear copper(II) complexes show a high catalytic activity. Dinuclear complexes also catalyse the oxidation process if the Cu···Cu distance is less than 5 Å. A steric match between substrate and complex is believed to be the determining factor: two metal centres have to be located in close proximity to facilitate binding of the two hydroxyl oxygen atoms of catechol prior to the electron transfer.[9a] This view is supported by the observation that dinuclear copper complexes are generally more reactive towards the oxidation of catechols than are corresponding mononuclear species.[9b,c] But so far only one crystal structure of a catalytically active dinuclear copper(II) complex with a co-ordinating catecholato ligand has been reported.[9d] No direct correlation between the rates of reaction and the redox potentials of complexes have been determined. Malachowski *et al.*[9e] have pointed out that a window of redox potentials for effective catalysis exists with a balance between ease of reduction by the substrate and subsequent reoxidation by molecular oxygen. Although some general correlations of structure–reactivity patterns have been found, the exploration of the oxidation chemistry of structurally well characterised copper complexes is still needed to fully understand the parameters affecting their catecholase activity.
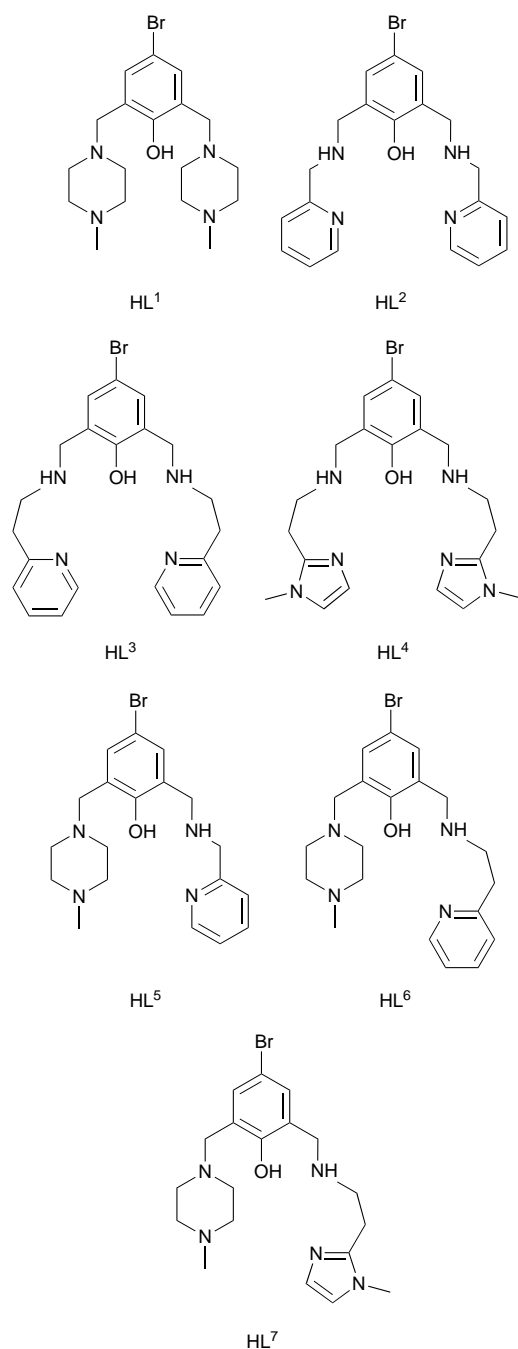

Fig. 1 Pentadentate dinucleating ligands employed for the syntheses of the complexes

In this work, we report on the synthesis of a series of dinuclear copper(II) complexes as potential structural and functional models for the active site of catechol oxidase. The design of the complexes is based (*a*) on the natural system, that means the active site of catechol oxidase, and (*b*) on the known structure–reactivity relationships. For this purpose, we synthesised pentadentate dinucleating ligands with a N_4O donor set (Fig. 1). The copper centres were expected to be bridged by the endogenous phenolate group of the ligand and by an exogenous hydroxide or alcoholate anion from the solvent, which should result in a Cu··· Cu distance of about 3 Å. In order to easily identify parameters possibly affecting the activity, we only performed small structural variations in the ligands within the series. These include chelate ring sizes, the nature of the nitrogen donors and the symmetry/non-symmetry of the pendant arms.

The symmetric ligand HL^1 is easily accessible in one step in a Mannich reaction. The other symmetric ligands HL^2–HL^4 were

obtained by a Schiff-base condensation of 4-bromo-2,6-diformylphenol with 2 equivalents of the appropriate primary amine followed by reduction with sodium tetrahydroborate. The asymmetric ligands were prepared using a route provided by Fenton and co-workers.[10] The asymmetric substituted phenol 5-bromo-2-hydroxybenzaldehyde serves as the starting material. The piperazine arm is introduced by a Mannich reaction. The aldehyde function is then treated with 1 equivalent of the appropriate primary amine and subsequently reduced to the secondary amine.

Experimental

Materials and methods

All reagents were purchased from commercial sources and used as received. If necessary solvents were dried by standard procedures. Proton NMR spectra were recorded on a Bruker WH 300 instrument; all chemical shifts are reported in parts per million (ppm) relative to an internal standard of tetramethylsilane. Electronic spectra were recorded on a Shimadzu UV-3100 spectrophotometer. Elemental analyses were performed on a Heraeus CHN-O-RAPID instrument. Cyclovoltammetric measurements were performed on a BAS CV-50W instrument in acetonitrile solution that was 0.1 mol dm^{-3} in tetrabutylammonium perchlorate and 10^{-3} mol dm^{-3} in metal complex at a glassy carbon electrode with an Ag–AgCl–3 mol dm^{-3} NaCl reference electrode and a platinum wire as the auxiliary electrode.

Ligand syntheses

4-Bromo-2,6-bis(hydroxymethyl)phenol,[11] 4-bromo-2,6-diformylphenol[12] and 2-(2-aminoethyl)-1-methylimidazole dihydrochloride[13] were prepared following published procedures. The ligand HL^1 is obtained analytically pure. The ligands HL^2–HL^7 are isolated as crude products but are sufficiently pure for the complex syntheses.

4-Bromo-2,6-bis(4-methylpiperazin-1-ylmethyl)phenol HL^1. The ligand was prepared according to a literature procedure.[14] 4-Bromophenol (5.19 g, 30 mmol), 1-methylpiperazine (7.77 cm^3, 70 mmol) and paraformaldehyde (2.10 g, 70 mmol) were dissolved in ethanol (60 cm^3) and refluxed for 24 h. After evaporation of the solvent the residue was treated with a 10% aqueous solution of sodium carbonate (30 cm^3) and subsequently extracted twice with diethyl ether (30 cm^3) and once with dichloromethane (30 cm^3). The combined organic phases were dried over sodium sulfate. After evaporation of the solvent a light yellow oil was obtained, which slowly crystallises upon standing. Yield: 9.20 g (23.2 mmol, 77%), m.p. 65–69 °C (Found: C, 54.07; H, 8.04; N, 14.05. C$_{18}$H$_{29}$BrN$_4$O requires C, 54.40; H, 7.36; N, 14.10%). ^{1}H NMR (CDCl$_3$): δ 2.29 (s, 6 H), 2.47 (br s, 8 H), 2.56 (br s, 8 H), 3.59 (s, 4 H), 7.17 (s, 2 H).

4-Bromo-2,6-bis[(2-pyridylmethyl)aminomethyl]phenol HL^2. 4-Bromo-2,6-diformylphenol (2.29 g, 10 mmol) was dissolved in warm ethanol (80 cm^3). 2-(Aminomethyl)pyridine (2.16 g, 20 mmol) was added and the solution was heated under reflux for 3 h. The resulting red solution was cooled in an ice–water bath, and sodium tetrahydroborate (1.01 g, 26.7 mmol) added in small portions. The suspension was stirred overnight and refluxed for 1 h. After cooling to room temperature the solution was treated with 12 mol dm^{-3} hydrochloric acid (4 cm^3) and vigorously stirred for 30 min. A pH of 8–9 was adjusted by addition of about 8 cm^3 of 5 mol dm^{-3} sodium hydroxide. Precipitated sodium borate was filtered off, and the volume of the filtrate reduced by evaporation. The residue was extracted with chloroform and dried over sodium sulfate. Evaporation of the solvent yielded an orange-red oil. Yield: 3.41 g (8.3 mmol, 83%) (Found: C, 54.99; H, 4.98; N, 12.68. C$_{20}$H$_{21}$BrN$_4$O requires C,

58.12; H, 5.12; N, 13.56%). ^{1}H NMR (CDCl$_3$): δ 3.89 (s, 4 H), 3.92 (s, 4 H), 7.13 (s, 2 H), 7.17 (m, 2 H), 7.27 (m, 2 H), 7.63 (m, 2 H), 8.56 (m, 2 H).

4-Bromo-2,6-bis{[2-(2-pyridyl)ethyl]aminomethyl}phenol HL^3. The procedure for the synthesis was analogous to the synthesis of HL^2 using 2-(2-aminoethyl)pyridine (2.45 g, 20 mmol). Yield: 3.56 g (8.1 mmol, 81%) of an orange oil (Found: C, 58.65; H, 5.83; N, 12.28. C$_{22}$H$_{25}$BrN$_4$O requires C, 59.87; H, 5.71; N, 12.69%). ^{1}H NMR (CDCl$_3$): δ 3.21 (m, 8 H), 4.06 (s, 4 H), 7.13 (m, 2 H), 7.16 (m, 2 H), 7.24 (s, 2 H), 7.62 (m, 2 H), 8.43 (m, 2 H).

4-Bromo-2,6-bis{[2-(1-methyl-2-imidazolyl)ethyl]amino-methyl}phenol HL^4. 2-(2-Aminoethyl)-1-methylimidazole di-hydrochloride (3.96 g, 20 mmol) and potassium hydroxide (2.24 g, 40 mmol) were dissolved in hot methanol (100 cm^3). Then 4-bromo-2,6-diformylphenol (2.29 g, 10 mmol) was added to the suspension (precipitated potassium chloride) and refluxed for 3 h. The residue which was obtained after evaporation of the solvent was taken up in dichloromethane (50 cm^3) and dried over sodium sulfate. After removal of the solvent under reduced pressure, the residue was dissolved in ethanol (50 cm^3). The Schiff base was reduced with sodium tetrahydroborate as described for the synthesis of HL^2. Yield: 3.62 g (8.1 mmol, 81%) of an orange oil (Found: C, 52.88; H, 6.29; N, 18.23. C$_{20}$H$_{27}$BrN$_6$O requires C, 53.69; H, 6.08; N, 18.79%). ^{1}H NMR (CDCl$_3$): δ 2.85 (t, 4 H), 3.07 (t, 4 H), 3.56 (s, 6 H), 3.89 (s, 4 H), 6.79 (d, 2 H), 6.90 (d, 2 H), 7.13 (s, 2 H).

4-Bromo-2-(4-methylpiperazin-1-ylmethyl)-6-[(2-pyridyl-methyl)aminomethyl]phenol HL^5. (*a*) 4-*Bromo-2-formyl-6-(4-methylpiperazin-1-ylmethyl)phenol*. The described procedure is a modification of a literature method.[10b] To a solution of 5-bromo-2-hydroxybenzaldehyde (24.12 g, 120 mmol) in warm ethanol (200 cm^3) was added 1-methylpiperazine (15.03 g, 150 mmol) and paraformaldehyde (4.50 g, 150 mmol). The reaction mixture was refluxed for 24 h. The volume of the solution was reduced by evaporation and the solution treated with a 5% aqueous solution of sodium carbonate (30 cm^3). The mixture was extracted four times with dichloromethane (25 cm^3) and the combined organic fractions dried over sodium sulfate. Evaporation of the solvent resulted in a red oil which was taken up in the minimum amount of hot dry diethyl ether. Upon cooling, the product crystallised as yellow needles. Yield: 18.84 g (60 mmol, 50%), m.p. 83–84 °C (Found: C, 49.81; H, 5.63; N, 8.87. Calc. for C$_{13}$H$_{17}$BrN$_2$O$_2$: C, 49.85; H, 5.47; N, 8.94%). ^{1}H NMR (CDCl$_3$): δ 2.32 (s, 3 H), 2.52 (br s, 4 H), 3.72 (s, 2 H), 7.37 (d, 1 H), 7.76 (d, 1 H), 10.29 (s, 1 H).
(*b*) 4-*Bromo-2-(4-methylpiperazin-1-ylmethyl)-6-[(2-pyridyl-methyl)aminomethyl]phenol HL^5*. To a solution of 4-bromo-2-formyl-6-(4-methylpiperazin-1-ylmethyl)phenol (18.79 g, 60 mmol) in ethanol (100 cm^3) was added 2-(aminomethyl)-pyridine (6.49 g, 60 mmol). The reaction mixture was refluxed for 3 h. Further synthesis and work-up was analogous to the described synthesis of HL^2. Yield: 19.21 g (48 mmol, 79%) of an orange-red oil (Found: C, 53.94; H, 6.06; N, 12.94. C$_{19}$H$_{25}$BrN$_4$O requires C, 56.35; H, 6.22; N, 13.82%). ^{1}H NMR (CDCl$_3$): δ 2.30 (s, 3 H), 2.48 (br s, 4 H), 2.52 (br s, 4 H), 3.64 (s, 2 H), 3.84 (s, 2 H), 3.93 (s, 2 H), 7.06 (d, 1 H), 7.15 (m, 1 H), 7.26 (d, 1 H), 7.32 (m, 1 H), 7.63 (m, 1 H), 8.55 (m, 1 H).

4-Bromo-2-(4-methylpiperazin-1-ylmethyl)-6-{[2-(2-pyridyl)-ethyl]aminomethyl}phenol HL^6. To a solution of 4-bromo-2-formyl-6-(4-methylpiperazin-1-ylmethyl)phenol (6.28 g, 20 mmol) in ethanol (65 cm^3) was added 2-(2-pyridyl)ethylamine (2.44 g, 20 mmol). The reaction mixture was refluxed for 3 h. Further synthesis and work-up was analogous to the described synthesis of HL^2. Yield: 6.21 g (14.8 mmol, 74%) of a yellow oil (Found: C, 56.65; H, 6.57; N, 13.19. C$_{20}$H$_{27}$BrN$_4$O requires C,

57.28; H, 6.49; N, 13.36%). ^{1}H NMR (CDCl$_3$): δ 2.30 (s, 3 H), 2.47 (br s, 4 H), 2.57 (br s, 4 H), 3.02 (m, 4 H), 3.62 (s, 2 H), 3.83 (s, 2 H), 7.07 (d, 1 H), 7.11 (m, 1 H), 7.17 (m, 1 H), 7.20 (d, 1 H), 7.59 (m, 1 H), 8.53 (m, 1 H).

4-Bromo-2-(4-methylpiperazin-1-ylmethyl)-6-{[2-(1-methyl-2-imidazolyl)ethyl]aminomethyl}phenol HL^7. 2-(2-Aminoethyl)-1-methylimidazole dihydrochloride (3.96 g, 20 mmol) and potassium hydroxide (2.24 g, 40 mmol) were dissolved in hot methanol (100 cm^3). Then 4-bromo-2-formyl-6-(4-methyl-piperazin-1-ylmethyl)phenol (6.26 g, 20 mmol) was added to the suspension (precipitated potassium chloride) and refluxed for 3 h. Further synthesis and work-up was analogous to the described synthesis of HL^4. Yield: 7.01 g (16.6 mmol, 83%) of a yellow viscous oil (Found: C, 50.62; H, 6.26; N, 14.44. C$_{19}$H$_{28}$BrN$_5$O requires C, 54.03; H, 6.68; N, 16.58%). ^{1}H NMR (CDCl$_3$): δ 2.31 (s, 3 H), 2.50 (br s, 4 H), 2.60 (br s, 4 H), 2.95 (t, 2 H), 3.14 (t, 2 H), 3.56 (s, 2 H), 3.64 (s, 2 H), 3.92 (s, 2 H), 6.79 (d, 1 H), 7.09 (d, 1 H), 7.25 (d, 1 H).

Complex syntheses

CAUTION: In general, perchlorate salts of metal complexes with organic ligands are potentially explosive. While none of the present perchlorate complexes has proved to be shock sensitive, care is recommended.

[Cu$_2$(L^1)(OH)(H$_2$O)(EtOH)][ClO$_4$]$_2$·H$_2$O 1. Copper(II) per-chlorate hexahydrate (185 mg, 0.50 mmol) and HL^1 (99 mg, 0.25 mmol) were dissolved in ethanol (10 cm^3). Addition of a few drops of triethylamine led to a colour change of the solution from green to green-blue. Upon standing for a few hours green-blue prismatic crystals precipitated, which were suitable for X-ray diffraction analysis. Yield: 110 mg (0.134 mmol, 54%) (Found: C, 29.00; H, 4.71; N, 6.87. C$_{20}$H$_{39}$BrCl$_2$Cu$_2$N$_4$O$_{13}$ requires C, 29.24; H, 4.79; N, 6.82%). UV/VIS (methanol): λ$_{max}$/nm (ε/dm^3 mol^{-1} cm^{-1}) 355 (2070), 633 (368).

[Cu$_2$(L^2)(OH)][NO$_3$]$_2$ 2. To a solution of copper(II) nitrate trihydrate (121 mg, 0.50 mmol) and HL^2 (103 mg, 0.25 mmol) in methanol (10 cm^3) was added isopropanol (20 cm^3). The complex was obtained as a green powder. Yield: 30 mg (0.044 mmol, 18%) (Found: C, 34.94; H, 3.24; N, 12.50. C$_{20}$H$_{21}$BrCu$_2$N$_6$O$_8$ requires C, 35.30; H, 3.11; N, 12.35%). UV/VIS (methanol): λ$_{max}$/nm (ε/dm^3 mol^{-1} cm^{-1}) 380–500 (sh), 643 (190).

[Cu$_2$(L^3)(OMe)(MeOH)(ClO$_4$)]ClO$_4$ 3. Copper(II) perchlor-ate hexahydrate (185 mg, 0.50 mmol) and HL^3 (110 mg, 0.25 mmol) were dissolved in methanol (20 cm^3). After the solution had been allowed to stand for a few hours, dark green rod-like crystals suitable for X-ray diffraction analysis were deposited. Yield: 98 mg (0.188 mmol, 47%) (Found: C, 33.71; H, 3.58; N, 6.65. C$_{24}$H$_{31}$BrCl$_2$Cu$_2$N$_4$O$_{11}$ requires C, 34.75; H, 3.77; N, 6.76%). UV/VIS (methanol): λ$_{max}$/nm (ε/dm^3 mol^{-1} cm^{-1}) 366 (3470), 613 (204).

[Cu$_2$(L^4)(OH)(MeOH)$_2$][BF$_4$]$_2$ 4. Copper(II) tetrafluoro-borate hydrate (128 mg, 0.50 mmol) and HL^4 (112 mg, 0.25 mmol) were dissolved in methanol (15 cm^3). After a few hours X-ray quality green-blue needles were deposited. Yield: 110 mg (0.133 mmol, 53%) (Found: C, 31.41; H, 4.13; N, 10.07. C$_{22}$H$_{35}$B$_2$BrCu$_2$F$_8$N$_6$O$_4$ requires C, 31.91; H, 4.26; N, 10.15%). UV/VIS (methanol): λ$_{max}$/nm (ε/dm^3 mol^{-1} cm^{-1}) 320–420 (sh), 646 (132).

[Cu$_2$(L^5)(OMe)][ClO$_4$]$_2$·2MeOH 5. Copper(II) perchlorate hexahydrate (185 mg, 0.50 mmol) and HL^5 (101 mg, 0.25 mmol) were dissolved in methanol (10 cm^3). A few drops of triethyl-amine were added, accompanied by a colour change from green to green-blue. After 1 d, small amounts of precipitate were filtered off. The product was obtained as a green-blue micro-

crystalline solid by gas-phase diffusion of diethyl ether into the solution. Yield: 37 mg (0.045 mmol, 18%) (Found: C, 31.63; H, 4.17; N, 6.79. $C_{22}H_{35}BrCl_2Cu_2N_4O_{12}$ requires C, 32.01; H, 4.27; N, 6.79%). UV/VIS (methanol): λ_{max}/nm (ε/dm^3 mol^{-1} cm^{-1}) 330–440 (sh), 627 (266).

[Cu$_2$(L^6)(OMe)(MeOH)(ClO$_4$)]ClO$_4$ 6. To a solution of copper(II) perchlorate hexahydrate (93 mg, 0.25 mmol) and HL^6 (52 mg, 0.125 mmol) in methanol (10 cm^3) was added a solution of sodium acetate trihydrate (34 mg, 0.25 mmol) in methanol (5 cm^3). After 1 d, small amounts of precipitate were filtered off. The product was obtained as dark green block-shaped crystals suitable for X-ray diffraction analysis by gas-phase diffusion of diethyl ether into the solution. Yield: 61 mg (0.075 mmol, 60%) (Found: C, 30.51; H, 3.59; N, 6.97. $C_{22}H_{33}BrCl_2Cu_2N_4O_{11}$ requires C, 32.73; H, 4.12; N, 6.94%). UV/VIS (methanol): λ_{max}/nm (ε/dm^3 mol^{-1} cm^{-1}) 355 (2700), 630 (280).

[Cu$_2$(L^7)(OMe)(MeOH)(ClO$_4$)]ClO$_4$ 7. Copper(II) perchlorate hexahydrate (185 mg, 0.50 mmol) and HL^7 (106 mg, 0.25 mmol) were dissolved in methanol (10 cm^3). A few drops of triethylamine were added, upon which the colour of the solution turned from green to green-blue. After 1 d, small amounts of precipitate were filtered off. Gas-phase diffusion of diethyl ether into the reaction mixture led to green-blue plate-like crystals of the product suitable for crystal-structure determination. Yield: 61 mg (0.075 mmol, 60%) (Found: C, 29.92; H, 3.86; N, 8.43. $C_{21}H_{34}BrCl_2Cu_2N_5O_{11}$ requires C, 31.12; H, 4.23; N, 8.64%). UV/VIS (methanol): λ_{max}/nm (ε/dm^3 mol^{-1} cm^{-1}) 342 (2090), 631 (252).

X-Ray crystallography

Intensity data for complexes **1** and **6** were collected on a Syntex P2$_1$ and a Siemens P3 four-cycle diffractometer, respectively (Mo-Kα, $\lambda = 0.710\,73$ Å, graphite monochromator), by using the ω-scan technique with a variable scan rate of 2.93–29.30° min^{-1}. The intensities of two reflections were monitored and no significant crystal deterioration was observed. An empirical absorption correction was applied (ψ scan). Intensity data for complexes **3**, **4** and **7** were collected on a STOE IPDS diffractometer (Mo-Kα, $\lambda = 0.710\,73$ Å, graphite monochromator) with a sample-to-plate distance of 60 mm and a scan range from 0 to 180° with an exposure time of 4 min per 1.5° increment for **3**, 5 min per 2.5° increment for **4**, and 3 min per 2.0° increment for **7**. A combined absorption and decay correction was applied (program DECAY [15]). Further data collection parameters are summarised in Table 1.

The structures were solved by using direct methods with the exception of **7**, which was solved by a Patterson synthesis (program XS [16]). A series of full-matrix least-squares refinement cycles on F^2 (program SHELXL 93 [17]) followed by Fourier syntheses gave all remaining atoms. The hydrogen atoms were placed at calculated positions, except for the positions of the hydrogen atoms bonded to the oxygen atoms O(2), O(3) and O(4) of the co-ordinated solvent molecules in **1**, which were taken from the Fourier map. The hydrogen atoms were constrained to 'ride' on the atom to which they are attached. The isotropic thermal parameters for the methyl and hydroxyl protons were refined with 1.5 times, and for all other hydrogen atoms with 1.2 times, the U_{eq} value of the corresponding atom. The non-hydrogen atoms were refined with anisotropic thermal parameters with the following exceptions of disordered atoms in the counter ions: the fluorine atoms F(5), F(6), F(7) and F(8) of the tetrafluoroborate in **4** and the oxygen atoms O(24A) and O(24B) of a perchlorate in **6**. The occupancy factors for the disordered atoms are 0.75(2) for F(1), F(2), F(3), F(4) and 0.25(2) for F(5), F(6), F(7), F(8) in **4**, and 0.48(1) for O(24A) and 0.52(1) for O(24B) in **6**.
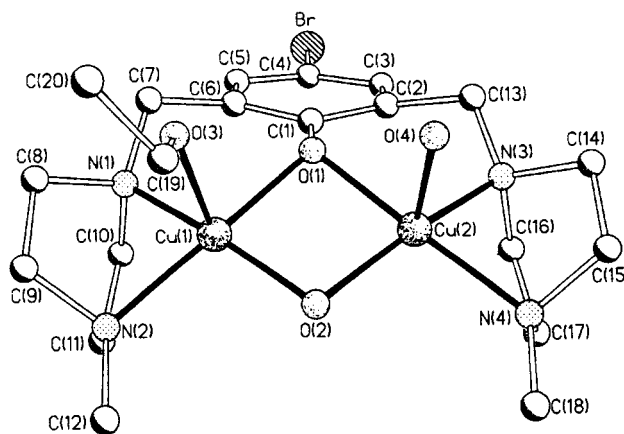
CCDC reference number 186/689.

Fig. 2 Molecular structure of the [Cu$_2$(L^1)(OH)(H$_2$O)(EtOH)]$^{2+}$ cation in **1** with the atomic numbering scheme. Hydrogen atoms are omitted for clarity

Catecholase activity study

The reaction of complexes **1**–**7** with 3,5-di-*tert*-butylcatechol (3,5-DTBC) was monitored as follows: 2 cm^3 of a 10^{-4} mol dm^{-3} solution of complex in methanol were treated with 0.1 cm^3 of a 0.1 mol dm^{-3} solution of 3,5-DTBC in methanol. The UV/VIS spectra of the original solution, of the solution directly after the addition and after 5, 10, 15 and 20 min were recorded and corrected for volume changes.

The titration of complexes **1**, **5**, **6** and **7** with tetrachlorocatechol (TCC) was carried out by adding 0.02 cm^3 aliquots of a 0.02 mol dm^{-3} solution of TCC to 2 cm^3 of a 2 × 10^{-4} mol dm^{-3} solution of complex in methanol. The thermodynamic equilibrium was reached immediately. The recorded spectra were corrected for volume changes.

Initial rates of catechol oxidation were determined by the following procedure. To 2 cm^3 of a methanolic solution of the complexes **1**, **5**, **6** and **7**, respectively, was added 0.1 cm^3 of a methanolic solution of 3,5-DTBC. The absorption at 400 nm was measured as a function of time over the first 2 min. The slope at $t = 0$ was used to calculate the rate. The mean value of three experiments was determined. The maximum deviation from the mean value did not exceed 10%.

Results and Discussion

Description of the crystal structures

The crystal structures of complexes **1**, **3**, **4**, **6** and **7** were determined. In general, all complexes consist of dinuclear cations in which the copper centres are bridged by the phenolate group [O(1)] of the respective deprotonated pentadentate ligand and an exogenous hydroxide or methanolate anion [O(2)]. The metal–metal distances vary between 2.874(1) and 3.002(1) Å. Each of the copper atoms has two nitrogen donors [N(1)–N(4)] of the ligand as terminal equatorial ligands. The axial positions are occupied by one or two solvent molecules or counter anions with elongated distances typical for Jahn–Teller distortion. The structures of the cations are shown in Figs. 2–6, selected interatomic distances and angles are given in Tables 2–6. Within the common structural motif, each of the complexes shows its own substantial characteristic features which is best documented in Fig. 7 showing projections of the cations along their O(2)–O(1) vectors.

[Cu$_2$(L^1)(OH)(H$_2$O)(EtOH)][ClO$_4$]$_2$·H$_2$O 1. The piperazine rings of [L^1]$^-$ are present in a boat conformation which is necessary to co-ordinate *via* both nitrogen atoms. Owing to the steric demand of this part of the ligand framework the angles N(1)–Cu(1)–N(2) and N(3)–Cu(2)–N(4) are unusually small [73.5(1) and 73.9(1)°, respectively] and deviate considerably

Table 1 Crystallographic data and experimental details

	1	**3**	**4**	**6**	**7**
Formula	$C_{20}H_{39}BrCl_2Cu_2N_4O_{13}$	$C_{24}H_{31}BrCl_2Cu_2N_4O_{11}$	$C_{22}H_{35}B_2BrCu_2F_8N_6O_4$	$C_{22}H_{33}BrCl_2Cu_2N_4O_{11}$	$C_{21}H_{34}BrCl_2Cu_2N_5O_{11}$
M	821.44	829.42	828.17	807.41	810.42
Crystal system	Monoclinic	Monoclinic	Orthorhombic	Monoclinic	Monoclinic
Space group	$P2_1/c$	$P2_1/n$	$Pbcn$	$P2_1/c$	$P2_1/c$
$a/\text{Å}$	16.913(3)	10.592(2)	16.043(3)	17.889(4)	17.349(3)
$b/\text{Å}$	11.046(2)	12.123(2)	12.689(3)	10.401(2)	8.828(2)
$c/\text{Å}$	16.617(3)	24.482(5)	15.810(3)	16.269(4)	19.797(4)
$\beta/°$	94.06(3)	92.97(3)	90	92.94(2)	94.04(3)
$U/\text{Å}^3$	3097	3139	3218	3023	3025
2θ Range/°	4.40–54.04	10.22–53.99	9.96–54.00	4.54–52.00	8.80–52.31
Lattice segment	$+h, +k, \pm l$	$\pm h, \pm k, \pm l$	$\pm h, \pm k, \pm l$	$+h, +k, \pm l$	$\pm h, \pm k, \pm l$
Z	4	4	4	4	4
T/K	150	213	213	170	213
$D_c/\text{g cm}^{-3}$	1.762	1.755	1.709	1.774	1.780
$F(000)$	1672	1672	1664	1632	1640
Crystal size/mm	$0.38 \times 0.25 \times 0.10$	$0.25 \times 0.10 \times 0.08$	$0.25 \times 0.08 \times 0.06$	$0.08 \times 0.25 \times 0.22$	$0.30 \times 0.25 \times 0.10$
Crystal shape and colour	Green-blue prisms	Dark green rods	Green-blue needles	Dark green blocks	Green-blue plates
μ/mm^{-1}	2.90	2.86	2.65	2.97	2.97
Unique data	6703	6694	3492	5831	5785
Observed data $[I > 2\sigma(I)]$	3699	4006	1748	3072	4434
Number of parameters	400	400	226	383	384
$R [I > 2\sigma(I)]$, [a] $R1$	0.0375	0.0730	0.0742	0.0612	0.0562
$wR2$	0.0672	0.1457	0.1195	0.1431	0.1360
R (all data),[a] $R1$	0.0814	0.1397	0.1831	0.1241	0.0796
$wR2$	0.0734	0.1868	0.1650	0.1630	0.1585
Weighting scheme, w^{-1} [b]	$[\sigma^2(F_o^2) + (0.0233P)^2]$	$[\sigma^2(F_o^2) + (0.0422P)^2 + 15.6529P]$	$[\sigma^2(F_o^2) + (0.0319P)^2 + 16.28P]$	$[\sigma^2(F_o^2) + (0.0891P)^2]$	$[\sigma^2(F_o^2) + (0.0594P)^2 + 9.2565P]$
Goodness of fit on F^2	0.753	1.079	1.065	0.896	1.079

[a] $R1 = \Sigma ||F_o| - |F_c||/\Sigma|F_o|$, $wR2 = [\Sigma w(F_o^2 - F_c^2)^2/\Sigma w(F_o^2)^2]^{\frac{1}{2}}$. [b] $P = (F_o^2 + 2F_c^2)/3$.

Fig. 3 Structure of $[Cu_2(L^3)(OMe)(MeOH)(ClO_4)]ClO_4$ **3** with the atomic numbering scheme. Hydrogen atoms are omitted for clarity

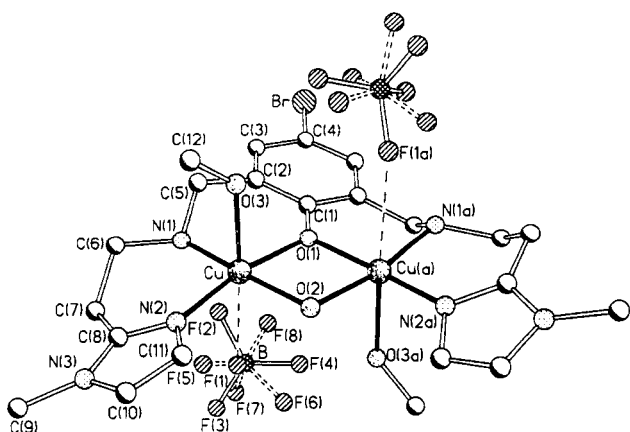**Fig. 4** Structure of $[Cu_2(L^4)(OH)(MeOH)_2][BF_4]_2$ **4** with the atomic numbering scheme. Hydrogen atoms are omitted for clarity
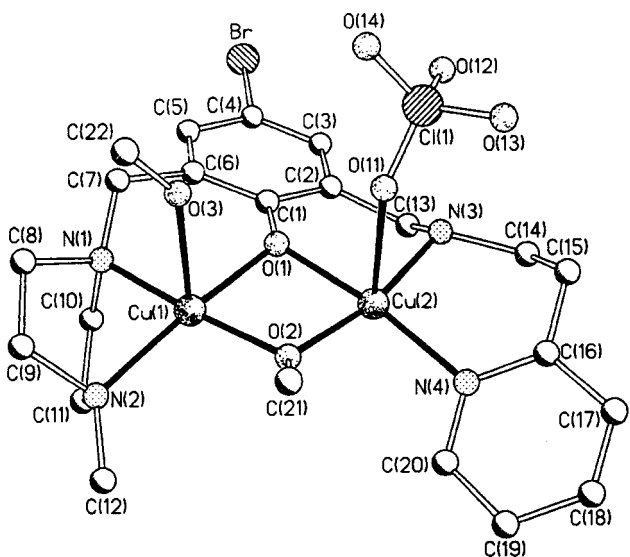

Fig. 5 Molecular structure of the $[Cu_2(L^6)(OMe)(MeOH)(ClO_4)]^+$ cation in **6** with the atomic numbering scheme. Hydrogen atoms are omitted for clarity

from the ideal 90°. This is compensated by the corresponding large angles O(2)–Cu(1)–N(2) and O(2)–Cu(2)–N(4) showing values of 103.7(1) and 103.9(1)°, respectively.

Table 2 Selected interatomic distances (Å) and angles (°) for complex **1**

Cu(1)–O(1)	1.996(2)	Cu(2)–O(1)	2.011(3)
Cu(1)–O(2)	1.927(3)	Cu(2)–O(2)	1.932(3)
Cu(1)–O(3)	2.227(3)	Cu(2)–O(4)	2.166(3)
Cu(1)–N(1)	1.979(3)	Cu(2)–N(3)	1.982(3)
Cu(1)–N(2)	2.063(3)	Cu(2)–N(4)	2.048(3)
Cu(1)···Cu(2)	2.902(1)		
Cu(1)–O(1)–Cu(2)	92.8(1)	Cu(1)–O(2)–Cu(2)	97.5(1)
O(1)–Cu(1)–O(2)	84.9(1)	O(1)–Cu(2)–O(2)	84.3(1)
O(1)–Cu(1)–O(3)	90.9(1)	O(1)–Cu(2)–O(4)	89.4(1)
O(1)–Cu(1)–N(1)	94.7(1)	O(1)–Cu(2)–N(3)	94.6(1)
O(1)–Cu(1)–N(2)	162.5(1)	O(1)–Cu(2)–N(4)	164.0(1)
O(2)–Cu(1)–O(3)	99.1(1)	O(2)–Cu(2)–O(4)	94.2(1)
O(2)–Cu(1)–N(1)	167.1(1)	O(2)–Cu(2)–N(3)	164.8(1)
O(2)–Cu(1)–N(2)	103.7(1)	O(2)–Cu(2)–N(4)	103.9(1)
O(3)–Cu(1)–N(1)	93.9(1)	O(4)–Cu(2)–N(3)	101.1(1)
O(3)–Cu(1)–N(2)	102.6(1)	O(4)–Cu(2)–N(4)	103.5(1)
N(1)–Cu(1)–N(2)	73.5(1)	N(3)–Cu(2)–N(4)	73.9(1)

Table 3 Selected interatomic distances (Å) and angles (°) for complex **3**

Cu(1)–O(1)	1.967(5)	Cu(2)–O(1)	1.931(5)
Cu(1)–O(2)	1.936(5)	Cu(2)–O(2)	1.925(5)
Cu(1)–O(3)	2.392(6)	Cu(2)–O(11)	2.640(5)
Cu(1)–O(10)	2.704(7)	Cu(2)···O(20)	3.207(8)
Cu(1)–N(1)	1.978(6)	Cu(2)–N(3)	2.009(6)
Cu(1)–N(2)	1.995(6)	Cu(2)–N(4)	1.961(6)
Cu(1)···Cu(2)	3.002(1)		
Cu(1)–O(1)–Cu(2)	100.7(2)	Cu(1)–O(2)–Cu(2)	102.1(2)
O(1)–Cu(1)–O(2)	77.6(2)	O(1)–Cu(2)–O(2)	78.7(2)
O(1)–Cu(1)–O(3)	87.9(2)	O(1)–Cu(2)–O(11)	82.2(2)
O(1)–Cu(1)–N(1)	89.1(2)	O(1)–Cu(2)–N(3)	93.0(2)
O(1)–Cu(1)–N(2)	169.7(2)	O(1)–Cu(2)–N(4)	169.8(2)
O(1)–Cu(1)–O(10)	88.4(2)	O(2)–Cu(2)–O(11)	89.9(2)
O(2)–Cu(1)–O(3)	93.3(2)	O(2)–Cu(2)–N(3)	166.5(3)
O(2)–Cu(1)–O(10)	89.6(2)	O(2)–Cu(2)–N(4)	95.0(2)
O(2)–Cu(1)–N(1)	166.7(2)	O(11)–Cu(2)–N(3)	99.6(2)
O(2)–Cu(1)–N(2)	96.8(2)	O(11)–Cu(2)–N(4)	89.9(2)
O(3)–Cu(1)–O(10)	174.7(2)	N(3)–Cu(2)–N(4)	94.6(2)
O(3)–Cu(1)–N(1)	85.4(3)		
O(3)–Cu(1)–N(2)	101.2(3)		
O(10)–Cu(1)–N(1)	90.8(2)		
O(10)–Cu(1)–N(2)	82.8(2)		
N(1)–Cu(1)–N(2)	96.4(2)		
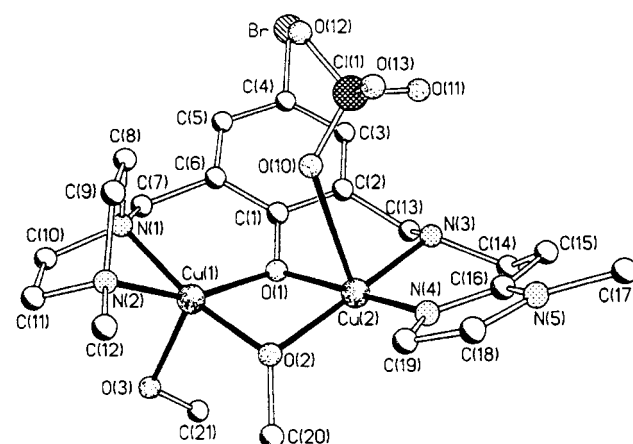
Fig. 6 Molecular structure of the $[Cu_2(L^7)(OMe)(MeOH)(ClO_4)]^+$ cation in **7** with the atomic numbering scheme. Hydrogen atoms are omitted for clarity

The calculation of the least-squares planes defined by the atoms of the square-planar co-ordination plane including the central atom shows the copper ions to be displaced from the basal planes towards the axial donors by 0.188(1) [Cu(1)] and

Table 4 Selected interatomic distances (Å) and angles (°) for complex **4***

Cu–O(1)	1.933(4)	Cu–O(2)	1.929(3)
Cu–O(3)	2.324(6)	Cu–N(1)	1.974(6)
Cu–N(2)	1.916(6)	Cu · · · F(1)	2.875(8)
Cu · · · Cu(a) *	2.995(2)		
Cu–O(1)–Cu(a) *	101.6(3)	Cu–O(2)–Cu(a) *	101.8(2)
O(1)–Cu–O(2)	78.3(2)	O(1)–Cu–O(3)	91.8(2)
O(1)–Cu–N(1)	92.8(2)	O(1)–Cu–N(2)	169.0(2)
O(2)–Cu–O(3)	89.7(2)	O(2)–Cu–N(1)	169.0(2)
O(2)–Cu–N(2)	92.5(2)	O(3)–Cu–N(1)	97.2(3)
O(3)–Cu–N(2)	94.2(3)	N(1)–Cu–N(2)	95.5(2)

* Symmetry transformation: $-x, y, 0.5 - z$.

Table 5 Selected interatomic distances (Å) and angles (°) for complex **6**
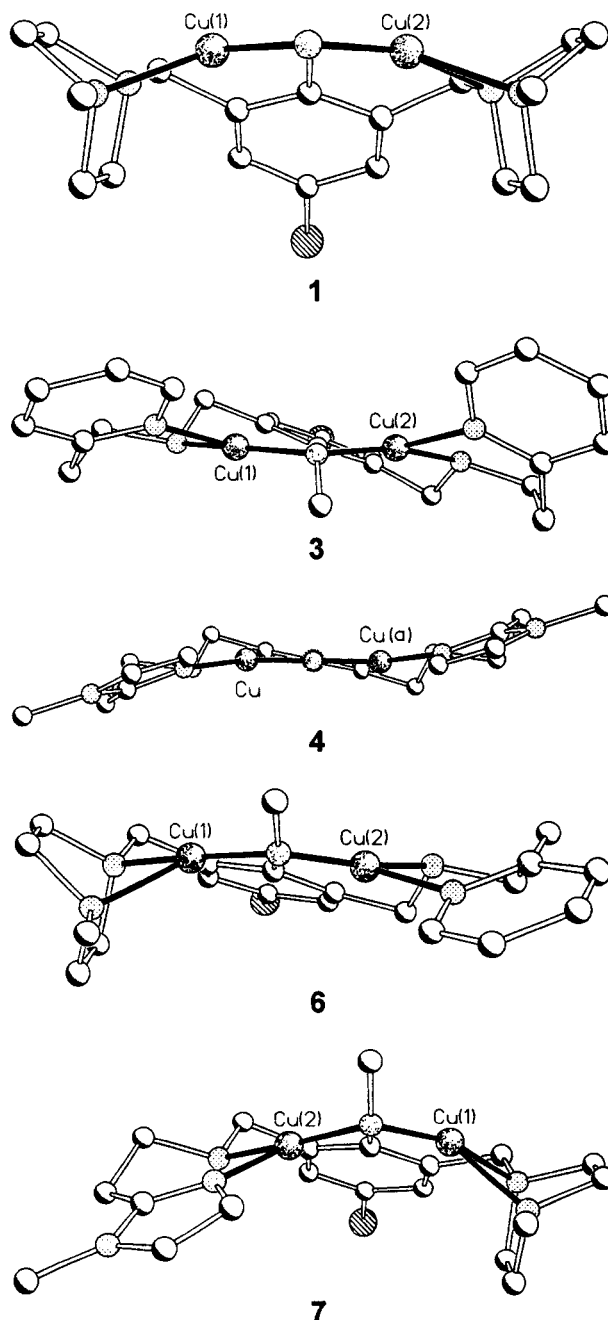
Cu(1)–O(1)	1.959(4)	Cu(2)–O(1)	1.958(4)
Cu(1)–O(2)	1.891(5)	Cu(2)–O(2)	1.911(5)
Cu(1)–O(3)	2.431(6)	Cu(2)–O(11)	2.615(7)
Cu(1)–N(1)	1.963(6)	Cu(2)–N(3)	1.980(7)
Cu(1)–N(2)	2.012(6)	Cu(2)–N(4)	1.999(6)
Cu(1) · · · Cu(2)	2.938(1)	Cu(2) · · · O(21)	3.031(16)
Cu(1)–O(1)–Cu(2)	97.2(2)	Cu(1)–O(2)–Cu(2)	101.2(2)
O(1)–Cu(1)–O(2)	80.5(2)	O(1)–Cu(2)–O(2)	80.0(2)
O(1)–Cu(1)–O(3)	87.0(2)	O(1)–Cu(2)–O(11)	86.5(3)
O(1)–Cu(1)–N(1)	95.0(2)	O(1)–Cu(2)–N(3)	89.6(2)
O(1)–Cu(1)–N(2)	156.2(2)	O(1)–Cu(2)–N(4)	171.6(2)
O(2)–Cu(1)–O(3)	91.5(2)	O(2)–Cu(2)–O(11)	84.8(2)
O(2)–Cu(1)–N(1)	175.1(2)	O(2)–Cu(2)–N(3)	168.6(2)
O(2)–Cu(1)–N(2)	108.2(2)	O(2)–Cu(2)–N(4)	94.3(2)
O(3)–Cu(1)–N(1)	90.1(2)	O(11)–Cu(2)–N(3)	89.8(3)
O(3)–Cu(1)–N(2)	114.3(3)	O(11)–Cu(2)–N(4)	99.3(3)
N(1)–Cu(1)–N(2)	75.3(3)	N(3)–Cu(2)–N(4)	96.5(3)

Table 6 Selected interatomic distances (Å) and angles (°) for complex **7**

Cu(1)–O(1)	1.975(4)	Cu(2)–O(1)	1.995(4)
Cu(1)–O(2)	1.885(4)	Cu(2)–O(2)	1.935(4)
Cu(1)–O(3)	2.274(5)	Cu(2)–O(10)	2.532(5)
Cu(1)–N(1)	1.984(5)	Cu(2)–N(3)	1.990(4)
Cu(1)–N(2)	2.043(5)	Cu(2)–N(4)	1.960(5)
Cu(1) · · · Cu(2)	2.874(1)		
Cu(1)–O(1)–Cu(2)	92.7(2)	Cu(1)–O(2)–Cu(2)	97.6(2)
O(1)–Cu(1)–O(2)	81.9(2)	O(1)–Cu(2)–O(2)	80.2(2)
O(1)–Cu(1)–O(3)	95.4(2)	O(1)–Cu(2)–O(10)	84.5(2)
O(1)–Cu(1)–N(1)	96.2(2)	O(1)–Cu(2)–N(3)	93.4(2)
O(1)–Cu(1)–N(2)	154.9(2)	O(1)–Cu(2)–N(4)	170.4(2)
O(2)–Cu(1)–O(3)	101.3(2)	O(2)–Cu(2)–O(10)	92.9(2)
O(2)–Cu(1)–N(1)	166.7(2)	O(2)–Cu(2)–N(3)	173.1(2)
O(2)–Cu(1)–N(2)	102.1(2)	O(2)–Cu(2)–N(4)	93.5(2)
O(3)–Cu(1)–N(1)	92.0(2)	O(10)–Cu(2)–N(3)	89.0(2)
O(3)–Cu(1)–N(2)	107.9(2)	O(10)–Cu(2)–N(4)	88.6(2)
N(1)–Cu(1)–N(2)	74.2(2)	N(3)–Cu(2)–N(4)	93.2(2)

Fig. 7 Projection of the cations of **1**, **3**, **4**, **6** and **7** along their O(2)–O(1) vectors (co-ordinating molecules or anions in axial positions are omitted)

0.192(1) Å [Cu(2)]. Although the angle between the two planes is 26.0(1)°, the central Cu_2O_2 moiety is essentially planar with a Cu(1)–O(1)–Cu(2)–O(2) dihedral angle of 5.1(1)°. The residues bound at the phenolate group have a *cis* conformation, meaning that the piperazine rings are located on the same side of the aromatic ring (see also Fig. 7). As a consequence, all atoms of the phenolate group lie on the same side of the Cu_2O_2 plane. The angle between the Cu_2O_2 and the aromatic ring plane is calculated to be 38.9(1)°. The phenolate oxygen O(1) adopts a trigonal-pyramidal geometry as can be expressed by the sum of the angles around O(1) which is 337.7(5)° and clearly smaller than 360°.

There is another striking aspect within the ligand molecule which can be attributed to the conformation of the ligand and so to the co-ordination to the metal centres: the methylene carbon atoms bound to the phenolate group are not in plane with the aromatic ring, they show unusually large displacements of 0.238(6) [C(7)] and 0.372(6) Å [C(13)].

$[Cu_2(L^3)(OMe)(MeOH)(ClO_4)]ClO_4$ 3. A least-squares calculation of the CuN_2O_2 planes reveals only relatively minor distortions for the basal plane of Cu(1): the deviations of the four donors lie in the range from 0.051(3) [N(1)] to 0.095(3) Å [O(1)], while the displacement of Cu(1) towards O(3) is 0.063(3) Å, and therefore in between these values and so of no significance. More notable distortions are observed for the basal plane of Cu(2): the donor atoms are displaced from the best plane by values between 0.129(3) [N(4)] and 0.166(3) Å [O(2)], while the central atom shows virtually no deviation [0.019(2) Å]. The angle between the two basal planes is 11.3(3)°, the central Cu_2O_2 unit is essentially planar as indicated by the Cu(1)–

O(1)−Cu(2)−O(2) dihedral angle of 6.8(2)°. In contrast to the situation in **1**, the residues bound at the bridging phenoxo group have a *trans* conformation. One half of the phenyl ring lies 'above', the other half 'beneath' the Cu_2O_2 plane (see also Fig. 7). The phenolate oxygen atom O(1) is in a trigonal-planar surrounding, the sum of angles is calculated to be 359(1)°.

[Cu₂(L⁴)(OH)(MeOH)₂][BF₄]₂ 4. A two-fold crystallographic axis passes through O(2), O(1), C(1), C(4) and Br; thus the co-ordination geometries around the two copper centres are identical. A least-squares calculation of the CuN_2O_2 plane shows that Cu lies only slightly [0.092(2) Å] above its basal plane in the direction of its axial ligand, O(3). The angle between the two least-squares planes around the copper centres is 0.5(2)°. For symmetry reasons, the central Cu_2O_2 unit forms an exact plane. The ligand possesses a *trans* conformation with respect to the aminomethyl groups and the phenol ring plane. The phenolate oxygen atom O(1) is exactly trigonal planar as indicated by the sum of angles which is calculated to be 360.0(5)°. Similar to **3**, one half of the phenol ring is 'above', the other half 'beneath' the central Cu_2O_2 moiety (see also Fig. 7).

[Cu₂(L⁶)(OMe)(MeOH)(ClO₄)]ClO₄ 6. The equatorial positions of each copper ion are occupied by two nitrogen donors of the asymmetric ligand [L⁶]⁻ arising in a non-equivalent environment for the metal centres. For Cu(1) these are two tertiary nitrogen atoms of the piperazine ring, for Cu(2) these are a secondary amine nitrogen and an aromatic pyridyl nitrogen donor. While the piperazine nitrogen atoms and Cu(1) are embedded in two five-membered chelate rings, Cu(2) and the nitrogen atoms N(1) and N(4) are part of a six-membered chelate ring. This results in significantly different N−Cu−N angles. Owing to the small bite of the piperazine group the angle N(1)−Cu(1)−N(2) is very small [75.3(3)°], in contrast to the angle N(3)−Cu(2)−N(4) which has a quite normal value of 96.5(3)°.

The square-planar basal plane of Cu(1) is strongly distorted. The plane defined by N(1), N(2) and Cu(1) is twisted toward the plane defined by O(1), O(2) and Cu(1) by an angle of 22.0(3)°. Calculation of the CuN_2O_2 least-squares plane of Cu(2) shows the basal plane of the pyramid also to be markedly distorted. The mean deviation of the atoms is 0.08 Å, but the central atom itself is only unessentially displaced in the direction of the axial perchlorate donor by 0.013(3) Å. The two CuN_2O_2 least-squares planes are tilted towards each other by 19.3(3)°. Nevertheless, the central Cu_2O_2 unit is nearly planar indicated by the Cu(1)−O(1)−Cu(2)−O(2) dihedral angle of 7.7(2)°. While in complex **1** the residues bound at the central μ-phenoxo bridge definitely assume a *cis* and in complex **3** a *trans* conformation, the situation in **6** is a mixture of both. Although, basically a *trans* conformation is found, the aromatic ring lies completely on one side of the central Cu_2O_2 plane which is characteristic for *cis* arrangements (see also Fig. 7). This is also expressed by the sum of angles around the phenolate oxygen atom O(1) which is 354.8(10)° indicating trigonal-pyramidal character.

[Cu₂(L⁷)(OMe)(MeOH)(ClO₄)]ClO₄ 7. The Cu(1) atom is co-ordinated by the tertiary aliphatic nitrogen atoms of the piperazine ring of [L⁷]⁻, Cu(2) is co-ordinated by the secondary aliphatic nitrogen function and the aromatic nitrogen donor of the methylimidazole group of [L⁷]⁻. Similar to **6**, this leads to a non-equivalency in the environment of the copper centres. Owing to the formation of two five-membered chelate rings, the angle N(1)−Cu(1)−N(2) [74.2(2)°] is remarkably contracted. The corresponding angle for Cu(2) N(3)−Cu(2)−N(4) is in a six-membered chelate ring and is therefore allowed to adopt an almost ideal value of 93.2(2)°.

The CuN_2O_2 basal plane of Cu(1) is considerably distorted.

A least-squares calculation shows a mean deviation of the four equatorial ligands from the best plane of about 0.10 Å with a displacement of the central atom towards the pyramid apex by 0.257(2) Å. The Cu(2) atom on the other hand shows much less distortion. The displacement of the copper centre by 0.035(2) Å is negligible in comparison to the mean deviation of the equatorial ligands from the best plane of about 0.08 Å. The two edge-shared co-ordination polyhedra are unusually strongly tilted toward each other by 41.8(1)°. Thereby, the central Cu_2O_2 unit in **7** is not planar which is expressed by the Cu(1)−O(1)−Cu(2)−O(2) dihedral angle of 20.0(2)°. The residues of the μ-phenoxo bridge adopt a *cis* conformation with respect to the phenol ring plane. All of the ring atoms lie on the same side of the least-squares plane defined by the Cu_2O_2 unit (see also Fig. 7). The phenolate oxygen atom O(1) is in a trigonal-pyramidal geometry with its neighbours C(1), Cu(1) and Cu(2), confirmed by the sum of angles of 341.7(8)°.

Discussion of the crystal structures

The compound [Cu₂(L)(OH)(H₂O)₂][ClO₄]₂·H₂O **1a**[19] is analogous to **1** and has been described by Murray and co-workers.[18] The difference between the ligand HL and HL¹ is the substituent in the position *para* to the phenol group, which is chloride in HL and bromide in HL¹. The cations of **1** and **1a** have essentially the same co-ordination geometries but differ in details. In the crystal of **1a** two crystallographically independent molecules are found both containing a mirror plane. Whereas in **1a** water molecules are bound to each of the copper centres, in **1** there is one water and one ethanol molecule resulting in an asymmetric co-ordination. In the compound studied in this work, the distances to these axial donors are about 0.1 Å shorter than in **1a** for which they are reported as 2.323(8) and 2.268(8) Å. Also in comparison to other copper(II) complexes, the axial bond lengths are very short, indicative of strong bonding. The Cu···Cu distances in **1a** were determined to be 2.872(2) and 2.857(3) Å, respectively, and are therefore significantly shorter than in **1**. Whereas in **1a** the dihedral angle between the phenol ring plane and the central Cu_2O_2 plane is reported to be 48.4 and 42.7°, respectively, in our compound it amounts to 38.9(1)°. Despite the use of analogous ligands, all of the described differences are significant and outside of estimated standard deviations. This cannot be ascribed simply to the influence of the *para* substituent of the phenolate bridge, because there are even deviations between the crystallographically independent complex molecules in the unit cell of **1a**. It seems to be more likely, that in the first line packing effects and the hydrogen-bonding network are responsible for the observed differences. For the synthesis of the complexes triethylamine was used as a base for **1** and sodium hydroxide for **1a**. The higher concentration of water in the reaction solution of **1a** may have led to the crystallisation of the complex molecule with two co-ordinated water molecules whereas **1** crystallises with one water and one ethanol molecule in the axial positions of the copper centres. Hence, despite similar co-ordinations there is a relatively broad range for bond distances and angles. It can be assumed, that the complexes show an enhanced flexibility in solution.

Recently, the complex [Cu₂L'(OH)]²⁺ **3a** has been reported as the product of a hydroxylation reaction (L' = 2,6-bis-{N-methyl-[2-(2-pyridyl)ethyl]aminomethyl}phenolate).[19] The main differences between this and the analogous compound **3** are the tertiary aliphatic amine donor instead of a secondary NH function and the hydroxo bridge instead of the methanolato bridge. The co-ordination geometries in the cation of **3** and **3a** are nearly identical considering the Cu···Cu distances [3.002(1) and 2.999(1) Å, respectively] and the dihedral angles [6.8(2) and 7.2(2)°, respectively] of the central Cu_2O_2 unit. All other bond lengths and angles differ only slightly. The dinuclear metal centre in **3** is bridged by a perchlorate anion. This

Table 7 Cyclic voltammetric data of the complexes

Complex	$E_{pc,1}$/V	$E_{pc,2}$/V	E_{pa}/V
1	−0.43	−0.72	+0.17
2	—	−0.83	+0.12
3	−0.51	−0.80	+0.18
4	−0.46	−0.72	+0.06
5	−0.38	−0.96	+0.13
6*	−0.37	−0.71	+0.17
7	−0.41	−0.79	+0.18

* $E_{pc,3}$ = −0.93 V.

structural motif is rather unusual and has so far been found in only a few dinuclear copper(II) complexes.[20]

In the syntheses of complexes **5**–**7** asymmetric ligands were employed. The crystal structures of **6** and **7** were determined. So far only three dicopper(II) complexes also containing pentadentate dinucleating ligands with μ-phenoxo bridge and a N_4O donor set have been characterised by X-ray crystallography.[10,21,22] These compounds are typical Schiff-base complexes. Hence, complexes **5**–**7** are the first asymmetric complexes within this series not containing an imine function.

The co-ordination geometries of the central atoms of the asymmetric complexes **6** and **7** correspond to those which are found for the metal centres in the corresponding symmetric complexes **1**, **3** and **4**. This means, in **6** and **7** Cu(1) is in a strongly distorted square-pyramidal environment dominated by the rigid piperazine ligand and which is also found in **1**. In **6** and **7** Cu(2) is surrounded by the more flexible [2-(2-pyridyl)ethyl]-amine and [2-(1-methyl-2-imidazolyl)ethyl]amine arms, respectively, forming six-membered chelate rings. The metals are allowed to form relatively minor distorted co-ordination polyhedra similar to those observed in **3** and **4**. In **1** the ligand has to possess a *cis* conformation with respect to the piperazine arms and the phenol ring plane to realise a μ-hydroxo bridged dicopper(II) centre. Owing to the higher flexibility of the ligands in **3** and **4**, they are found in the more favourable *trans* conformation. It is interesting, that in **6** and **7** different compromises were followed to balance the unlike steric constraints of both ligand frameworks. In **6** the piperazine arm and the [2-(2-pyridyl)ethyl]amine residue are arranged in a *trans* conformation. This unfavourable solution for the piperazine part leads to the observed twist within the basal plane of Cu(1). On the contrary, the ligand in **7** adopts a *cis* conformation. As a consequence, the basal planes of the copper atoms are extremely tilted: the angle between both least-squares planes is calculated to be 41.8(1)°, the dihedral angle within the Cu_2O_2 moiety is 20.0(2)°. This is the reason for the very short metal–metal separation of 2.874(1) Å. It is difficult to understand why the analogous ligands HL^6 and HL^7 have chosen these different co-ordination patterns. The conformation observed in **6** could also be realised in **7** and *vice versa*. Possibly, an equilibrium of two (or more) conformers exists in solution.

The dinuclear copper complexes **1**, **3**, **4**, **6** and **7** represent good structural models for the active sites of the met forms of catechol oxidases. The complexes simulate the short copper–copper distance of about 3 Å as well as the N_2O_2 donor set, which is formed in the enzymes by two imidazoles of the amino acid histidine and the di(μ-hydroxo) bridge.[8]

Electrochemical properties

Cyclic voltammograms were recorded in the potential range from +1.00 to −1.00 V *vs.* Ag–AgCl in acetonitrile (starting value: +1.00 V). The scan rate was 0.20 V s^{-1} in all cases, with the exception of **2** and **4**, which were measured at a scan rate of 0.30 V s^{-1}. Table 7 gives the obtained peak potentials.

The cyclic voltammograms of all of the studied complexes reveal irreversible and ill defined cathodic reduction peaks in the range from −0.37 to −0.96 V. In the cyclic voltammogram

of **6** three reduction peaks are observed whereas for the other complexes two peaks appear. The cyclic voltammogram of **2** contains particularly broad peaks, so that the first 'peak' is observed as a weak shoulder in the range from about 0 to −0.3 V. These reduction peaks are assigned to the one-electron processes $Cu^{II}Cu^{II} \longrightarrow Cu^{II}Cu^I$ and $Cu^{II}Cu^I \longrightarrow Cu^ICu^I$. In the case of **6** it has to be assumed that the third peak is due to a further reduction to Cu^0. All of the complexes exhibit a broad anodic oxidation peak in the range from +0.06 to +0.18 V. The breadth of this peak suggests a superposition of two close one-electron processes, which are assigned to the reoxidations to the $Cu^{II}Cu^I$ and $Cu^{II}Cu^{II}$ species, respectively.

These observations are typical for μ-hydroxo bridged dicopper(II) complexes and have been found in electroanalytical studies of similar or analogous compounds.[18b,20h,23] Irreversibility of redox processes in metal complexes in electrochemical experiments are attributed to changes in the co-ordination geometry or co-ordination number (*e.g.* solvent co-ordination/dissociation) upon change of the oxidation state or even to the expulsion of metal ions from the co-ordination sphere.[24] Hydroxo bridges have a poor ability to bind to (electrogenerated) Cu^I centres,[23c,25] which should also be the case for alkoxo bridges. Therefore, the OH$^-$ and OMe$^-$ bridges, respectively, are expected to dissociate from the co-ordination sphere upon reduction. Due to the different preferred co-ordination polyhedra of Cu^I and Cu^{II} it is further expected that considerable changes of the co-ordination geometry occur. Association of acetonitrile is not unlikely because of its high binding tendency towards Cu^I. On the whole, it can be postulated that the structure of the Cu^ICu^I species (or even the Cu^ICu^{II} species) differs notably from the structure of the original $Cu^{II}Cu^{II}$ complex. Considerable structural changes occur again upon reoxidation. However, a reassociation to the original hydroxo or methanolato bridged copper(II) complex is most unlikely: the chance for a combination of the reoxidised $Cu^{II}Cu^{II}$ species with the previously dissociated oxo bridge within the cyclovoltammetric experiment is extremely low. This assumption is confirmed by the fact that in a second scan the shape and position of the reduction peaks change. The irreversible charge-transfer processes in the cyclovoltammetric experiments do not completely exclude the applicability of the complexes as oxidation catalysts. The fact that the complexes are able to be reoxidised is decisive.

Catecholase activity study and kinetics

In most of the catecholase activity studies of model complexes 3,5-di-*tert*-butylcatechol (3,5-DTBC) has been employed as the substrate. The product, 3,5-di-*tert*-butyl-*o*-quinone (3,5-DTBQ), is considerably stable and has a strong absorption at λ_{max} = 400 nm (ε = 1900 dm^3 mol^{-1} cm^{-1}).[9a] Therefore, activities and reaction rates, respectively, can be determined using electronic spectroscopy by following the appearance of the absorption maximum of the quinone. The reactivity studies were performed in methanol solution because of the good solubility of the complexes as well as of the substrate and of its product.

Prior to a detailed kinetic study, it is necessary to get an estimation of the ability of the complexes to oxidise catechol. For this purpose, 10^{-4} mol dm^{-3} solutions of **1**–**7** in methanol were treated with 50 equivalents of 3,5-DTBC in the presence of air. The course of the reaction was followed by UV/VIS spectroscopy over the first 20 min. The first apparent result is that the reactivities of the complexes differ significantly from each other. Whereas **1** and the unsymmetric complexes **5**–**7** show a comparatively high catecholase activity, the symmetric complexes **2**–**4** show only little or no activity. Complex **1** has the highest catecholase activity of all complexes in this study. After 5 min an increase in absorption at 400 nm of about 1.4 units is observed, which means a turnover of more than seven equiv-
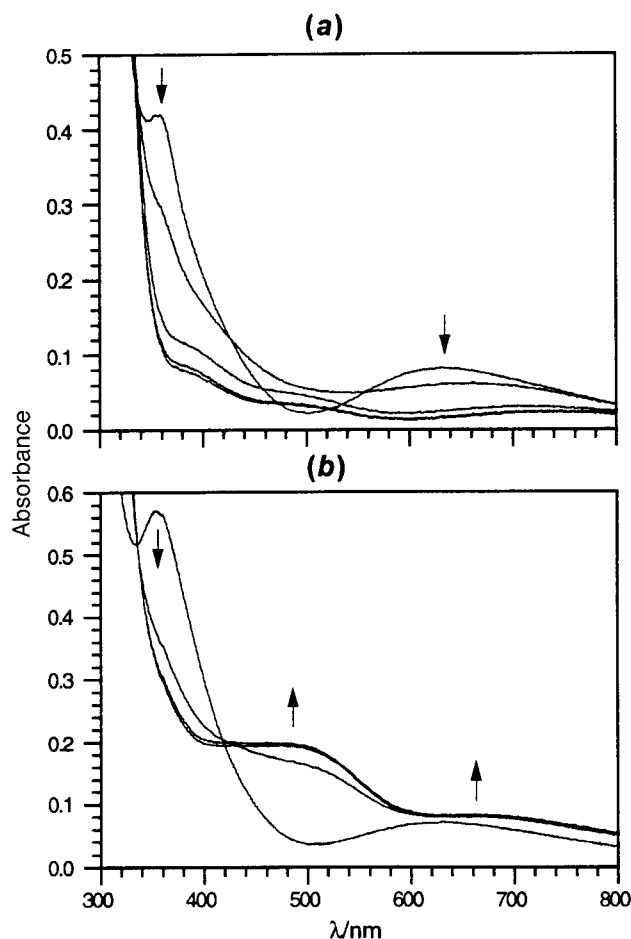
Fig. 8 (*a*) The UV/VIS spectra of the titration of **1** ($c = 2 \times 10^{-4}$ mol dm^{-3}) with 1, 2 and 3 equivalents of TCC; (*b*) UV/VIS spectra of the titration of **6** ($c = 2 \times 10^{-4}$ mol dm^{-3}) with 1 and 2 equivalents of TCC

transfer transition, the lower energy band is possibly due to a catecholate $\longrightarrow$ Cu^{II} charge transfer.[9d] The corresponding titrations of **5**, **6** and **7** differ considerably from the one just described, but among themselves they show an analogous behaviour towards TCC. Fig. 8(*b*) shows the UV/VIS spectra of the titration of **6** with TCC. In this case the end of the titration is reached after addition of 2 equivalents of TCC. The maximum of the charge-transfer band at 355 nm disappears, concomitantly a broad plateau-like band evolves between 400 and 500 nm ($\varepsilon \approx 1000$ dm^3 mol^{-1} cm^{-1}). This absorption can be interpreted as a superposition of the phenolate and the catecholate $\longrightarrow$ Cu^{II} charge-transfer transition. The intensity of the d–d bands increases slightly and also a plateau-like maximum is formed between 600 and 700 nm ($\varepsilon \approx 400$ dm^3 mol^{-1} cm^{-1}). On the contrary, addition of TCC to solutions of the inactive complexes **2**, **3** and **4** leads to only insignificant changes of their UV/VIS spectra. Thus, binding of TCC to the copper centres of the active complexes is evident, whereas the inactive complexes seem to be indifferent towards TCC.

The kinetics of the oxidation of 3,5-DTBC were determined by the method of initial rates by monitoring the growth of the 400 nm band of the product 3,5-DTBQ. A linear relationship for the initial rates and the complex concentration is obtained for complexes **1**, **5**, **6** and **7**, meaning a first-order dependence on the catalyst concentration for the four systems. To determine the dependence of the rates on the substrate concentration, solutions of the complexes **1**, **5**, **6** and **7** were treated with varying amounts of 3,5-DTBC. At low concentrations of 3,5-DTBC (stoichiometric or slightly higher) a first-order dependence of the substrate concentration was observed. At higher concentrations, a saturation kinetics was found for all four compounds. A treatment on the basis of the Michaelis–Menten model, originally developed for enzyme kinetics, was applied. In our case, we can also propose a pre-equilibrium of free complex and substrate on the one hand, and a complex–substrate adduct on the other hand. The irreversible conversion into complex and quinone can be imagined as the rate-determining step. Although a much more complicated mechanism may be involved, the results show this simple model to be sufficient for a kinetic description.

For the determination of the kinetic parameters for **1** the substrate concentration was varied in the range from 2.41×10^{-4} to 4.51×10^{-3} mol dm^{-3} at a complex concentration of 4.76×10^{-5} mol dm^{-3}. The concentration of **5**, as well as of **6** and **7**, was adjusted to 9.52×10^{-5} mol dm^{-3}. The substrate concentration was varied between 1.88×10^{-3} and 1.13×10^{-2} mol dm^{-3}. For **6** a variation of substrate concentration between 4.77×10^{-4} and 9.34×10^{-3} mol dm^{-3} was chosen, and for **7** the corresponding range was 9.24×10^{-4} to 9.39×10^{-3} mol dm^{-3}. Table 8 contains the results evaluated from Lineweaver–Burk plots.

Conclusion

A series of dinuclear copper(II) complexes has been synthesised. The copper centres are μ-phenoxo bridged by a pentadentate dinucleating ligand and further have an exogenous μ-hydroxo or μ-methanolato bridge. They differ by the employed terminal

alents of 3,5-DTBC. Complexes **6**, **7** and **5** have significantly lower activities and can be graduated in this order: the increase of absorption at 400 nm after 20 min can be expressed in turnovers of 10.7, 7.0 and 5.3, respectively. Hence, these complexes show catalytic activity. Complex **2** possesses a negligibly low catecholase activity (turnover of 0.6 after 20 min). A detailed kinetic analysis is therefore dispensable. The catecholase activity of **3** is even lower, and **4** is essentially inactive.

It is remarkable, that the addition of 50 equivalents of 3,5-DTBC to the inactive complexes has nearly no influence on their UV/VIS spectra. The bands in the charge-transfer region as well as the d–d bands remain unchanged with respect to position and intensity. Therefore, binding of 3,5-DTBC to the dinuclear copper(II) centre can be definitely excluded. Owing to the developing product bands in the UV/VIS spectra of the active complexes, it is difficult to make clear statements about the co-ordination of catechol to the metal centre. Hence, the complexes were titrated with tetrachlorocatechol (TCC). Owing to its electron withdrawing substituents, this *o*-diphenol has a high redox potential and is not oxidised by the copper complexes. Fig. 8(*a*) shows the UV/VIS spectra of the titration of a 2×10^{-4} mol dm^{-3} solution of **1** with TCC. The original spectrum changes dramatically upon addition of TCC. After addition of 3 equivalents, the end of the titration is reached. In the charge-transfer region of about 340–450 nm the intensity decreases, simultaneously a new weak band appears at about 500 nm. The maximum of the d–d bands shifts from 633 to 725 nm accompanied by a drastic decrease of the absorption coefficient to 125 dm^3 mol^{-1} cm^{-1}. The two bands at about 400 nm ($\varepsilon \approx 370$ dm^3 mol^{-1} cm^{-1}) and 500 nm ($\varepsilon \approx 170$ dm^3 mol^{-1} cm^{-1}) reveal unexpected low intensities. The higher energy band can presumably be assigned to a phenolate $\longrightarrow$ Cu^{II} charge-

nitrogen donors within the ligand. For the symmetric complexes two piperazine units (**1**), two (2-pyridylmethyl)amine units (**2**), two [2-(2-pyridyl)ethyl]amine units (**3**) and two [2-(1-methyl-2-imidazolyl)ethyl]amine units (**4**) were used. For the asymmetric complexes a combination of one piperazine unit and one of the other three mentioned functional groups were employed. The structures of the complexes **1**, **3**, **4**, **6** and **7** could be obtained by X-ray crystallography. They represent good structural models for the active sites of the met forms of catechol oxidases. They simulate the short Cu⋯Cu distance of about 3 Å as well as the N_2O_2 donor set and the Cu_2O_2 central unit.

The investigation of the catecholase activity of compounds **1**–**7** revealed that only the symmetric complex **1** and the asymmetric complexes **5**–**7** have significant catalytic activity with respect to the aerial oxidation of 3,5-DTBC to its corresponding *o*-quinone. The decisive thermodynamic property determining an electron-transfer reaction is the redox potential of each reactant. The electrochemical behaviour of the complexes was investigated in acetonitrile solution revealing only irreversible and ill defined reduction steps. The potentials for the oxidation of 3,5-DTBC to its corresponding semiquinone and quinone have been reported.[26] These potentials are very sensitive to the degree of protonation and/or the number of transferred electrons. No clear relationship between the electrochemical properties of the complexes and the reported data for 3,5-DTBC exists. It may be that the poorly defined redox chemistry of this class of complexes will never allow such a correlation to be established.

The common characteristic of the active complexes is the co-ordinating piperazine group within their ligand framework. This distinguishes the active complexes from the inactive ones. Obviously, this structural unit is essential for catecholase activity of the studied series of complexes. The crystal structures have revealed that the square-pyramidal co-ordination geometries of the copper ions in **1**, **5**, **6** and **7** are strongly distorted, and that for the dinuclear cations on the whole a strained structure results. The symmetric complexes **2**, **3** and **4** on the contrary are present in a relaxed, energetically favoured conformation. This leads to the assumption that the differences in reactivity are primarily based on geometric factors.

Complex **1** is definitely the most strained system of all of the complexes synthesised in this work. This strain is caused by the exogenous μ-hydroxo bridge forcing the rigid ligand framework to assume an unfavoured conformation. In the presence of alternative bridging co-ordination partners with a larger bite distance, the complex will adopt a relaxed conformation. This is shown by the crystal structure of a dinuclear bis(μ-acetato)-bridged copper(II) complex of a ligand which is analogous to HL^1.[18b] Therefore, **1** is willing to give up the μ-hydroxo bridged structural motif in favour of a bridging catechol co-ordination. This is surely also valid for complexes **5**–**7**, although in a weakened sense. Binding of catechol was proven by spectroscopic titration with TCC. In contrast to this, complexes **2**–**4** are completely indifferent towards catechol. Even in the presence of a large excess of 3,5-DTBC no binding is observed. The structural motif of a μ-hydroxo and μ-alkoxo bridged dicopper(II) centre, respectively, is obviously significantly more stable than a bridging catechol co-ordination. However, co-ordination of catechol is a necessary condition for electron transfer to the copper centres.

The distinct gradation of oxidation rates of the active compounds is in accord with the gradation of strain within the complexes. For the most strained complex **1** a turnover number of 214 h^{-1} was determined, for the less strained systems of **5**, **6** and **7** values between 33 and 48 h^{-1} were obtained. Also in accord with this view is the correlation of k_{cat} with the Michaelis–Menten constant K_M (see Table 8): higher activity goes along with a lower K_M value, *i.e.* a more stable complex–substrate adduct.

References

1 J. Haggin, *Chem. Eng. News*, 1993, **71**, 23; L. I. Simándi, in *Catalytic Activation of Dioxygen by Metal Complexes*, Kluwer Academic Publishers, Dordrecht, Boston, London, 1992.

2 S. J. Lippard and J. M. Berg, *Principles of Bioinorganic Chemistry*, University Science Books, Mill Valley, CA, 1994; W. Kaim and B. Schwederski, *Bioinorganic Chemistry*, John Wiley and Sons, Chichester, 1994.

3 W. Kaim and J. Rall, *Angew. Chem.*, 1996, **108**, 47; *Angew. Chem., Int. Ed. Engl.*, 1996, **35**, 43; T. G. Spiro, *Copper Proteins*, John Wiley and Sons, New York, 1981; E. I. Solomon, K. W. Penfield and D. E. Wilcox, *Struct. Bonding*, (*Berlin*), 1983, **53**, 1; K. D. Karlin and Z. Tyeklár, *Bioinorganic Chemistry of Copper*, Chapman and Hall, New York, London, 1993.

4 K. A. Magnus, H. Ton-That and J. E. Carpenter, *Chem. Rev.*, 1994, **94**, 727; J. Ling, L. P. Nestor, R. S. Czernuszewicz, T. G. Spiro, R. Fraczkiewicz, K. D. Sharma, T. M. Loehr and J. Sanders-Loehr, *J. Am. Chem. Soc.*, 1994, **116**, 7682.

5 K. Lerch, *Life Chem. Rep.*, 1987, **5**, 221; H. S. Mason, W. L. Fowlks and E. Peterson, *J. Am. Chem. Soc.*, 1955, **77**, 2914.

6 M. Trémolières and J. B. Bieth, *Phytochemistry*, 1984, **23**, 501.

7 D. Meiwes, B. Ross, M. Kiesshauer, K. Cammann, H. Witzel, M. Knoll, M. Borchardt and C. Sandermaier, *Lab. Med.*, 1992, **15**, 24.

8 (*a*) A. Rompel, K. Büldt, B. Krebs, H. Fischer, D. Meiwes, H. Witzel, H.-F. Nolting and C. Hermes, *Hamburg Synchrotron Laboratory* (*HASYLAB*) *Annual Report*, 1993, p. 691; (*b*) A. Rompel, Ph.D. Dissertation, University of Münster, 1993; (*c*) F. Zippel, F. Ahlers, B. Krebs, S. Behning, K. Büldt-Karentzopoulos, H. Witzel and M. Oversluizen, *Daresbury Annual Report*, Daresbury Laboratory, Daresbury, 1994/1995, p. 102; (*d*) A. Rompel, H. Fischer, K. Büldt-Karentzopoulos, D. Meiwes, F. Zippel, H.-F. Nolting, C. Hermes, B. Krebs and H. Witzel, *J. Inorg. Biochem.*, 1995, **59**, 715; (*e*) B. Krebs, K. Büldt-Karentzopoulos, C. Eicken, A. Rompel, H. Witzel, A. Feldmann, R. Kruth, J. Reim, W. Steinforth, S. Teipel, F. Zippel, S. Schindler and F. Wiesemann, in *Bioinorganic Chemistry: Transition Metals in Biology and their Coordination Chemistry*, ed. A. X. Trautwein, VCH, Weinheim, 1997, ch. D.14, pp. 616–631, in the press.

9 Representative examples: (*a*) N. Oishi, Y. Nishida, K. Ida and S. Kida, *Bull. Chem. Soc. Jpn.*, 1980, **53**, 2847; (*b*) U. Casellato, S. Tamburini, P. A. Vigato, A. de Stefani, M. Vidali and D. E. Fenton, *Inorg. Chim. Acta*, 1983, **69**, 45; (*c*) M. R. Malachowski and M. G. Davidson, *Inorg. Chim. Acta*, 1989, **162**, 199; (*d*) K. D. Karlin, Y. Gultneh, T. Nicholson and J. Zubieta, *Inorg. Chem.*, 1985, **24**, 3727; (*e*) M. R. Malachowski, H. B. Huynh, L. J. Tomlinson, R. S. Kelly and J. W. Furbee, jun., *J. Chem. Soc., Dalton Trans.*, 1995, 31; (*f*) F. Zippel, F. Ahlers, R. Werner, W. Haase, H.-F. Nolting and B. Krebs, *Inorg. Chem.*, 1996, **35**, 3409.

10 (*a*) H. Adams, G. Candeland, J. D. Crane, D. E. Fenton and A. J. Smith, *J. Chem. Soc., Chem. Commun.*, 1990, 93; (*b*) J. D. Crane, D. E. Fenton, J.-M. Latour and A. J. Smith, *J. Chem. Soc., Dalton Trans.*, 1991, 2979.

11 J. Leroy and C. Wakselman, *J. Fluorine Chem.*, 1988, **40**, 23.

12 Ru-Gang Xie, Zhu-Jun Zhang, Jia-Ming Yan and De-Qi Yuan, *Synth. Commun.*, 1994, **24**, 53.

13 A. Buschauer and W. Schunack, *Arch. Pharm.* (*Weinheim*), 1983, **316**, 891.

14 J. H. Hodgkin, *Aust. J. Chem.*, 1984, **37**, 2371.

15 STOE IPDS software package, STOE & CIE, Darmstadt, 1993.

16 G. M. Sheldrick, SHELXTL PLUS, Siemens Analytical X-Ray Instruments, Madison, WI, 1990.

17 G. M. Sheldrick, SHELXL 93, Program for Crystal Structure Determination, University of Göttingen, 1993.

18 (*a*) G. D. Fallon, K. S. Murray, B. Spethmann, J. K. Yandell, J. H. Hodgkin and B. C. Loft, *J. Chem. Soc., Chem. Commun.*, 1984, 1561; (*b*) K. Bertoncello, G. D. Fallon, J. H. Hodgkin and K. S. Murray, *Inorg. Chem.*, 1988, **27**, 4750.

19 D. Ghosh, T. K. Lal, S. Ghosh and R. Mukherjee, *Chem. Commun.*, 1996, 13.

20 (*a*) A. M. García, J. Manzur, M. T. Garland, R. Baggio, O. Gonzáles, O. Peña and E. Spodine, *Inorg. Chim. Acta*, 1996, **248**, 247; (*b*) S. Schindler, D. J. Szalda and C. Creutz, *Inorg. Chem.*, 1992,

31, 2255; (*c*) S. K. Mandal, L. K. Thompson, M. J. Newlands and E. J. Gabe, *Inorg. Chem.*, 1989, **28**, 3707; (*d*) Tian-Huey Lu, Hsi-Chi Shan, Min-Shium Chao and Chung-Sun Chung, *Acta Crystallogr.*, *Sect. C*, 1987, **43**, 207; (*e*) C. J. O'Connor, D. Firmin, A. K. Pant, B. R. Babu and E. D. Stevens, *Inorg. Chem.*, 1986, **25**, 2300; (*f*) P. Iliopoulos, G. D. Fallon and K. S. Murray, *J. Chem. Soc.*, *Dalton Trans.*, 1986, 437; (*g*) P. K. Coughlin and S. J. Lippard, *J. Am. Chem. Soc.*, 1981, **103**, 3228; (*h*) S. K. Mandal, L. K. Thompson, K. Nag, J.-P. Charland and E. J. Gabe, *Inorg. Chem.*, 1987, **26**, 1391.

21 M. Lubben, R. Hage, A. Meetsma, K. Bÿma and B. L. Feringa, *Inorg. Chem.*, 1995, **34**, 2217.

22 M. Andruh, O. Kahn, J. Sainton, Y. Dromzee and S. Jeannin, *Inorg. Chem.*, 1993, **32**, 1623.

23 (*a*) P. Zanello, S. Tamburini, P. A. Vigato and G. A. Mazzocchin, *Coord. Chem. Rev.*, 1987, **77**, 165; (*b*) J. J. Grzybowski, P. H. Merrell and F. L. Urbach, *Inorg. Chem.*, 1978, **17**, 3078; (*c*) R. R. Gagné, R. P. Kreh and J. A. Dodge, *J. Am. Chem. Soc.*, 1979, **101**, 6917; (*d*) S. K. Mandal and K. Nag, *J. Chem. Soc.*, *Dalton Trans.*, 1984, 2141.

24 S. Karunakaran and M. Kandaswamy, *J. Chem. Soc.*, *Dalton Trans.*, 1995, 1851.

25 L. Casella, O. Carugo, M. Gullotti, S. Garofani and P. Zanello, *Inorg. Chem.*, 1993, **32**, 2056.

26 M. D. Stallings, M. M. Morrison and D. T. Sawyer, *Inorg. Chem.*, 1981, **20**, 2655; S. Harmalker, S. E. Jones and D. T. Sawyer, *Inorg. Chem.*, 1983, **22**, 2790.